A polarization maintaining optical fiber Bragg grating multi-parameter sensor

YAGE ZHAN, KAN GU, JUN LUO, HUA WU*, MUHUO YU
State Key Laboratory for Modification of Chemical Fibers and Polymer Materials, Donghua University, Shanghai 201602, P.R. China

A polarization maintaining optical fiber Bragg grating (PMFBG) sensor with multi-parameter monitoring functions for composite structure has been studied theoretically and experimentally. A single embedded PMFBG is used as the sensor head for multi-parameter real-time monitoring in glass fiber reinforced polymer (GFRP) laminates. The temperature and stress response characteristics of the PMFBG in GFRP have been studied. The two peak wavelengths in the reflection spectrum of the PMFBG shift linearly with the temperature and/or stress of the laminates. Furthermore, the temperature sensitivity of the peak wavelengths of the PMFBG improve from 10.2m/℃ to 17.8pm/℃ (x-axis) and from 9. 6 pm/℃ to 15.1 pm/℃ (y-axis) after embedded in the composite laminates. The axial stress and temperature of the GFRP can be interrogated according to the two different wavelength shifts of the two peaks in the reflection spectrum. According to the experimental results, a single PMFBG sensor is competent for temperature and stress real-time monitoring simultaneously for composite structure.

(Received October 14, 2011; accepted February 20, 2012)

Keywords: Optical fiber multi-parameter sensor, Polarization maintaining fiber Bragg grating (PMFBG), Temperature, Stress

1. Introduction

Composite materials are applied to primary load-bearing structures in various industries because of their good specific stiffness and strength. Composite has been with rapid development and widespread use in recent years. However, deformation, cracks and other damages of most composite structure will emerge mainly due to extreme stress, abnormal temperature during long-term service. These damages have some impact on the performance of the structures and bring latent hazard. Therefore, structure health monitoring (SHM) is very important. Traditional detection methods for SHM, such as ultrasonic C-scan, optical interference, radiation, are difficult to achieve real-time monitoring. Most traditional methods are complex, high cost, electromechanical and susceptible to electromagnetic interference, which limits practical application.

Fiber grating sensors have many special advantages, such as small size, high sensitivity, electromagnetic interference resistance, corrosion resistance. These advantages make fiber grating sensor becoming one of the most promising sensor [1].

A Bragg grating sensors embedded in composites are an alternative solution for conventional dielectric sensors for composite structure [2]. One parameter, such as strain of composites has been monitored with fiber grating sensors in the curing process of autoclave molding process [3,4]. Strain in the laminates with different laying methods has been monitored in the curing course and the effect of laying method on the strain has been analyzed [5,6]. Temperature, pressure or stress of composite structure has been monitored using a common Bragg grating sensor [7]. Furthermore, fiber grating sensors have been used for damage detection in carbon fiber reinforced polymer (CFRP) delimitation [8]. However, it is unavailable to measure multi-parameters by one common FBG sensor. The system will be complex and high-cost if the multi-parameters of composite structure are measured with several FBGs or several other optic fiber components [9].

In this paper, a multi-parameter sensor based on an embedded PMFBG has been studied theoretically and experimentally. PMFBG is embedded in GFRP laminates through vacuum-assisted resin transfer molding (VARTM) process. Experiment results indicate that a single PMFBG is competent for monitoring temperature and strain simultaneously.

2. Principle

When the temperature and/or axial strain of a common FBG changes, the shift of its peak wavelength can be expressed as [9]:

$$\Delta\lambda_B = \lambda_B \cdot [(\alpha_0 + \beta_0) \cdot \Delta T + (1 - P_\varepsilon) \cdot \Delta\varepsilon] \tag{1}$$

where λ_B and $\Delta\lambda_B$ are the original peak wavelength and its shift respectively. α_0 and β_0 are thermal-expansion coefficient and thermo-optic coefficient of the optical fiber. P_e is effective elastic-optic coefficient, ΔT and $\Delta\varepsilon$ are temperature variation and axial strain variation. For common silica fiber, α_0, β_0 and P_e are constants. $\Delta\lambda_B$ has a good linear relationship with the temperature and/or axial strain of the FBG.

Ignoring the coupling of the two polarization models, when a FBG is written into polarization maintaining optical fiber, a PMFBG will be generated. The reflection spectrum of the PMFBG can be considered as the sum of two different FBGs and there are two peaks in the reflection spectrum of the PMFBG, as shown in Fig. 1. The wavelengths of the two peaks are determined by the effective refractive indexes of the fast axis (x-axis) and the slow axis (y-axis) of the fiber. The peak wavelengths are expressed as [10]:

$$\lambda_P^x = 2\Lambda n_{eff}^x \quad (2)$$

$$\lambda_P^y = 2\Lambda n_{eff}^y \quad (3)$$

where Λ is the grating period. n_{eff}^x and n_{eff}^y are effective refractive indexes of x-axis and y-axis respectively. The two refractive indexes are different, so the two peak wavelength are separated and the sensitivities of them to temperature and strain are different. Therefore, the temperature and the axial stress can be monitored simultaneously by a single PMFBG.

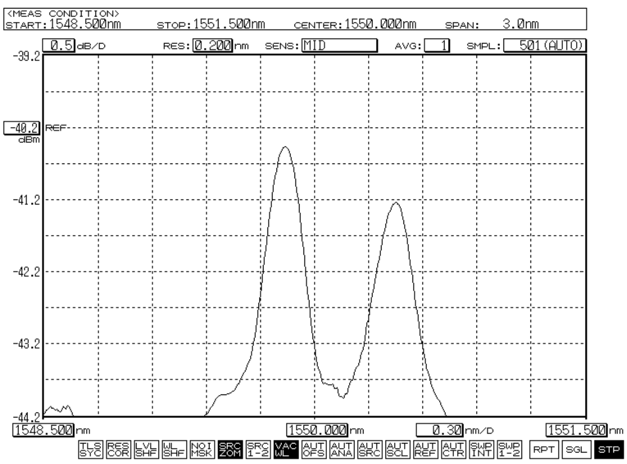

Fig.1 The reflection spectrum of the PMFBG.

3. Experiment and results

3.1 The preparation of specimens

Glass fiber fabric is used as reinforced fiber in the specimens. Epoxy resin is used as the matrix. The epoxy resin is mixed with polyamide curing agent at a weight ratio of 100:75. The curing cycle is constituted by a heating ramp of 5°/min and a thermostatic duration of 2 hours at 80°, followed by another 2 hours at 120°, finally natural cooling.

The GFRP lamination specimens are fabricated through VARTM process, with dimensions of 200×44×2.5mm^3. If the fiber grating is embedded in 90º direction, the cross-points which are resulted from the optical fiber and the reinforcing fibers can lead to stress concentration and the resin-rich region. When embedded in 0º direction, the influence is reduced to a minimum. Therefore, The specimens are designed to [0º/90º/0º(FBG)0º/90º/0º] and [0º/90º/0º(FPM)0º/90º/0º], a total of 6 layers. The PMFBG was embedded in the GFRP laminates, as shown in Fig. 2.

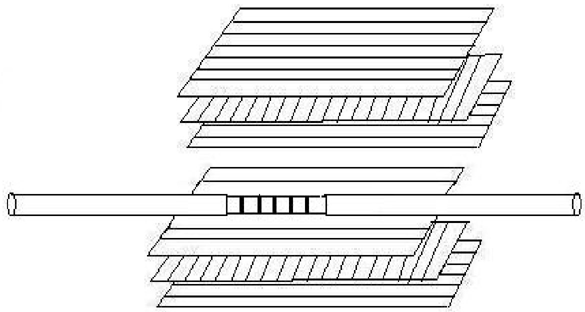

Fig. 2 The schematic diagram of the specimen.

Micron Optics SM125 optical sensing interrogator was used for the wavelength interrogation. The WDW3020 micro-controlled electronic universal testing machine was used for stress test. The setups of the experiment are shown in Fig. 3.

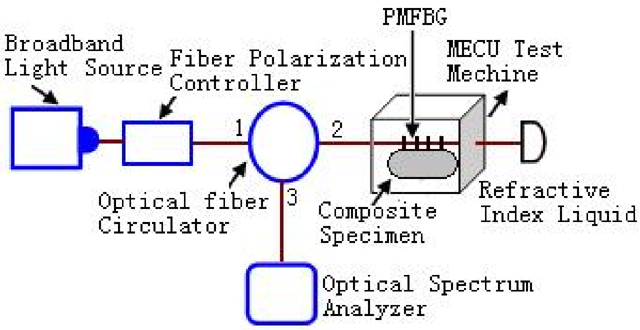

Fig. 3 Schematic diagram of the experiment setup.

3.2. Experiment results

3.2.1 The results of temperature experiment

The temperature-wavelength coefficients of the PMFBG are measured before and after embedded into the GFRP. The experiment data and the fitting curves are shown in Figs. 4 and 5.

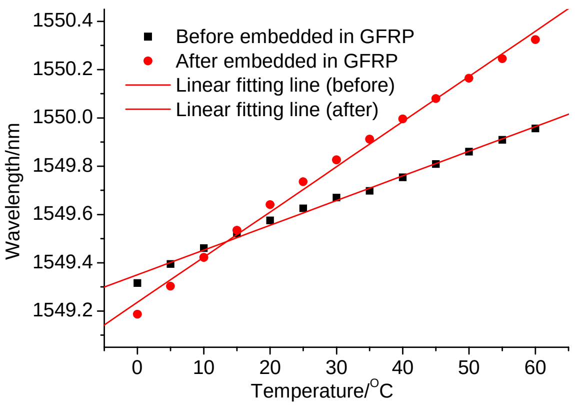

Fig.4 The peak wavelengths of PMFBG in x-axis shift with temperature.

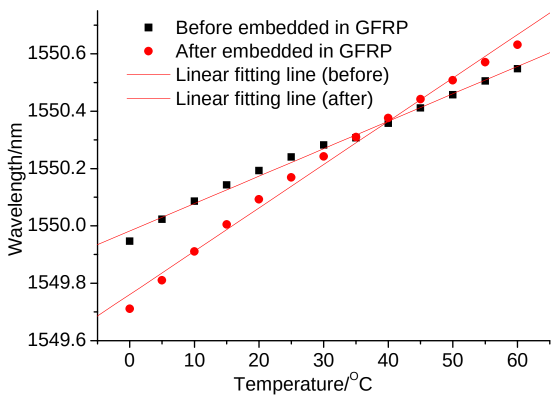

Fig. 5 The peak wavelengths of PMFBG in y-axis shift with temperature.

Figs. 4 and 5 show that the two peak wavelengths of the PMFBG (x-axis, y-axis) all shift linearly with the temperature, whether before or after embedded in GFRP. The linear fitting equations with respect to the peak wavelength in x-axis are $\lambda_{x(0)} = 0.0102T + 1549.3510$ before embedded in GFRP and $\lambda_{x(1)} = 0.0178T + 1549.2001$ after embedded in GFRP. The fitting degrees are 0.9971 and 0.9967 respectively. The linear fitting equations with respect to the peak wavelength in y-axis are $\lambda_{y(0)} = 0.0096T + 1549.9824$ before embedded in GFRP and $\lambda_{y(1)} = 0.0151T + 1549.7710$ after embedded in GFRP. The fitting degrees are 0.9962 and 0.9960 respectively.

There are large improvements of temperature sensitivities of both peak wavelengths in x-axis and in y-axis after embedded into GFRP. The temperature sensitivities of PMFBG improve from 10.2m/℃ to 17.8pm/℃ in x-axis and form 9.6 pm/℃ to 15.1 pm/℃ in y-axis respectively. The experimental results are repeatable.

The temperature-wavelength sensitivities of the two peaks in x-axis and y-axis of the PMFBG are not identical with each other, which is benefit to multi-parameter measurement and to distinguish the cross-sensitivity between the parameters.

3.2.2 The results of stress experiment

The stress of the PMFBG is implemented by stretching the GFRP using WDW3020 micro-controlled electronic universal testing machine with a step speed of 2.5mm/min. The peak wavelengths of the PMFBG are recorded by SM125 optical sensing interrogator. The temperature remains 3℃ during experiments. The experiment data and the fitting curves are shown as below.

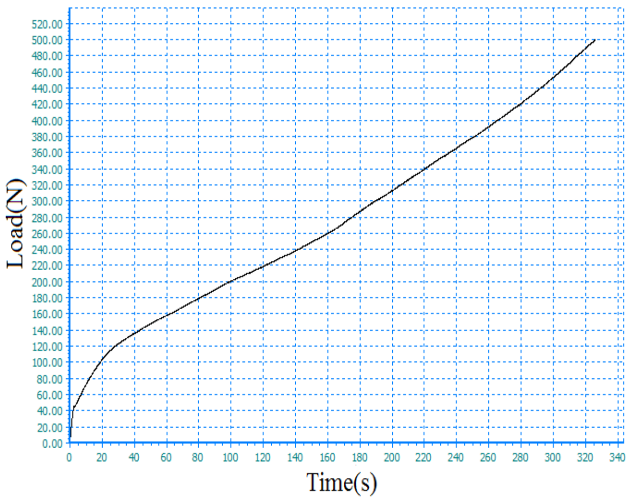

Fig. 6. The load added to the GFRP during experiment.

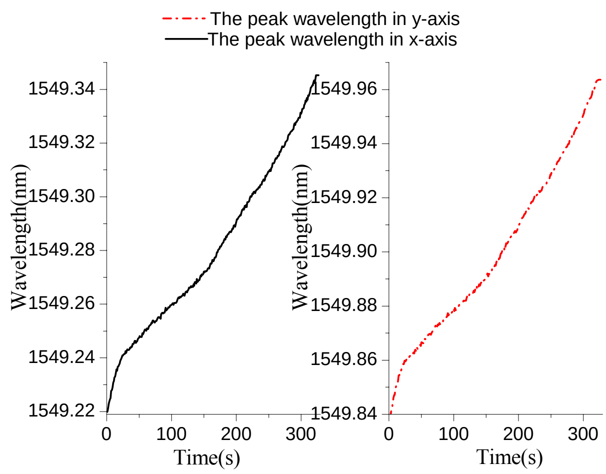

Fig. 7. The two peak wavelengths shifting process of PMFBG during experiment.

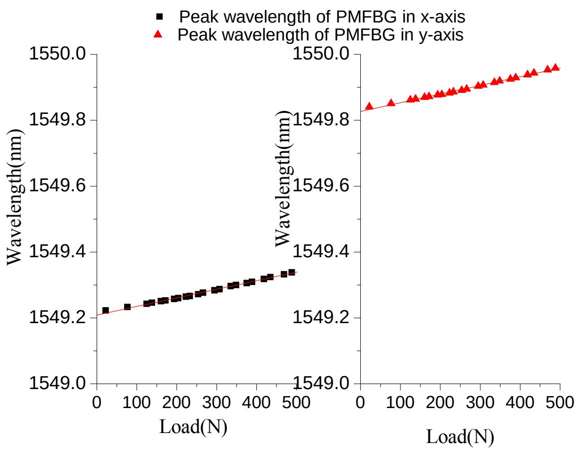

Fig. 8. The peak wavelength of the PMFBG shifting with the tensile load.

According to Figs. 6, 7 and 8, the two peak wavelengths of the PMFBG all shift linearly with the tensile load. The linear fitting equations for the two wavelengths in x-axis and y-axis are $\lambda_{x(F)} = 2.61\times10^{-4}F + 1549.21$ and $\lambda_{y(F)} = 2.64\times10^{-4}F + 1549.83$, respectively. The fitting degrees are 0.9980 and 0.9980 respectively.

According to the tensile load and the dimensions of the specimen, the stress of the GFRP and also the axial stress of the PMFBG can be calculated. In experiments, the stress of the GFRP specimen was in its elastic deformation stage, and its stress is regarded being proportional to the tensile load. According to the experiment data, the two peak wavelengths of the PMFBG all shift linearly with its stress. Therefore the stress of the GFRP can be real-time monitored by the PMFBG sensor. The two peak wavelengths of the PMFBG show different stress-wavelength sensitivities.

4. Discussions

The relationship between the stress of the composites and its strain within elastic deformation scope is expressed as Eq.4:

$$\sigma = E\frac{\Delta L}{L} = E\varepsilon \qquad (4)$$

The variation of λ_P of the PMFBG resulted from the axial strain is determined as:

$$\Delta\lambda_P = \lambda_P\left\{1-\frac{n^2}{2}[\rho_{12}-\nu(\rho_{11}-\rho_{12})]\right\}\cdot\varepsilon = \lambda_P\cdot[1-P_e]\cdot\varepsilon \qquad (5)$$

ρ_{11} and ρ_{12} are stress tensor components of the optical fiber, ν is Poisson's ratio. For common quartz fiber, $P_e \approx 0.222$. According to the experiment data, for example, λ_P^y is 1549.83nm with 4.6N load to the GFRP and is 1549.97nm with 546.7N load to the GFRP, all at the temperature of 3℃. The Young modulus of composite structure is estimated as follow:

$$\frac{F}{S} = E\cdot\frac{\Delta\lambda_P}{\lambda_P(1-P_e)} \qquad (6)$$

$$E = \frac{(F_2-F_1)\cdot\lambda_B(1-P_e)}{S\cdot(\lambda_{P,2}^y-\lambda_{P,1}^y)} \approx 42.4GPa \qquad (7)$$

The theoretical Young modulus's range of the GFRP is 40GPa. The measured value of the Young modulus GFRP is 41GPa. Therefore, the experiment results agree with the practical performance of the GFRP.

According to Eq.2 and Eq.3, the shift of the two peak wavelengths in x-axis and y-axis are expressed as:

$$\Delta\lambda_x = k_{x,\varepsilon}\cdot\Delta\varepsilon + k_{x,T}\cdot\Delta T \qquad (8)$$

$$\Delta\lambda_y = k_{y,\varepsilon}\cdot\Delta\varepsilon + k_{y,T}\cdot\Delta T \qquad (9)$$

where $k_{x,\varepsilon}$ and $k_{x,T}$ are coefficients for strain-wavelength sensitivity and temperature-wavelength sensitivity of the x-axis peak of the PMFBG. $k_{y,\varepsilon}$ and $k_{y,T}$ are coefficients for strain-wavelength sensitivity and temperature-wavelength sensitivity of the y-axis peak of the PMFBG. According to experiment results, $k_{x,\varepsilon}$ is approximately equal to $k_{y,\varepsilon}$, and $k_{x,T}$ is not equal to $k_{y,T}$ with a major difference. Therefore, by solving equations of Eq.8 and Eq.9, stress and temperature of the GFRP can be monitored with a single PMFBG. On the other hand, with the temperature increasing, the two peak wavelengths in the reflection spectrum of the PMFBG all increase but the separation between the two peaks decreases. From the results of stress experiment, with the stress increasing, the two peak wavelengths in the reflection spectrum all increase but the separation between the two peaks almost not change.

5. Conclusions

A multi-parameter composite sensor based on an embedded polarization maintaining optical fiber Bragg grating (PMFBG) for composite structure has been theoretically analyzed and experimentally confirmed. The experimental results show that the temperature sensitivities of the PMFBG have been improved significantly after embedded into GFRP. The wavelength of the PMFBG embedded into GFRP has a linear relationship with the stress. The two peaks in the reflection spectrum of the PMFBG are different in the temperature response and the stress response. Two parameters (such as temperature and strain) of the composite structure can be monitored simultaneously by demodulating the two peak wavelengths of the PMFBG with a single PMFBG.

Acknowledgments

Supported by Natural Science Foundation of China (50903014) and the Fundamental Research Funds for the Central University.

References

[1] T. J. Wang, CH. Wu, L. J. Lee, Polymer Composites **15**, 2978 (1994).
[2] M. J. Dwyer, G. M. Maistros, S. W. James, R. P. Tatam, I. K. Partridgez, Measur. Sci. Technol. **9**, 1153 (1998).
[3] V. M. Murukeshan, P. Y. Chan, L. S. Song, Sensors and Actuators:A. **79,** 153(2000)
[4] A. L.Kalamkarov, S. B. Fitzgerald, D. O. MacDonald. Composites: PartB. **30,** 753 (1999).
[5] C. M. Lawrence, D. V. Nelson, J. R. Spingarn, SPlE. **2718**, 60 (1996).
[6] J. S. Leng, A. Asundi: Smart. Mater. Struct. **11**, 249 (2002).
[7] Z. J. Wu, B. M. Zhang, L. B. Wan: Composites. **21**, 82 (2004).
[8] N. Takedaa, Y. Okabe, J. Kuwahara, S. Kojimac, T. Ogisud, Compos. Sci. Technol. **65**, 2575 (2005).
[9] Z. F. Bucholt, Electronics Letters.**12**, 122 (1994).
[10] Z. A. Jia, X. G. Qiao, Optoelectronic Laser **14,** 453 (2003).

*Corresponding author: wuhua@dhu.edu.cn